THE JOURNAL OF BIOLOGICAL CHEMISTRY
Vol. 276, No. 21, Issue of May 25, pp. 18038–18045, 2001

Printed in U.S.A.

A Plant 3′-Phosphoesterase Involved in the Repair of DNA Strand Breaks Generated by Oxidative Damage*

Received for publication, November 26, 2000, and in revised form, February 19, 2001
Published, JBC Papers in Press, February 27, 2001, DOI 10.1074/jbc.M010648200

Marco Betti, Stefania Petrucco, Angelo Bolchi, Giorgio Dieci, and Simone Ottonello‡

From the Istituto di Scienze Biochimiche, Università di Parma, I-43100 Parma, Italy

Two novel, structurally and functionally distinct phosphatases have been identified through the functional complementation, by maize cDNAs, of an *Escherichia coli* diphosphonucleoside phosphatase mutant strain. The first, ZmDP1, is a classical Mg^{2+}-dependent and Li^{+}-sensitive diphosphonucleoside phosphatase that dephosphorylates both 3′-phosphoadenosine 5′-phosphate (3′-PAP) and 2′-PAP without any discrimination between the 3′- and 2′-positions. The other, ZmDP2, is a distinct phosphatase that also catalyzes diphosphonucleoside dephosphorylation, but with a 12-fold lower Li^{+} sensitivity, a strong preference for 3′-PAP, and the unique ability to utilize double-stranded DNA molecules with 3′-phosphate- or 3′-phosphoglycolate-blocking groups as substrates. Importantly, ZmDP2, but not ZmDP1, conferred resistance to a DNA repair-deficient *E. coli* strain against oxidative DNA-damaging agents generating 3′-phosphate- or 3′-phosphoglycolate-blocked single strand breaks. ZmDP2 shares a partial amino acid sequence similarity with a recently identified human polynucleotide kinase 3′-phosphatase that is thought to be involved in DNA repair, but is devoid of 5′-kinase activity. ZmDP2 is the first DNA 3′-phosphoesterase thus far identified in plants capable of converting 3′-blocked termini into priming sites for reparative DNA polymerization.

Diphosphonucleoside phosphatases (DPNPases)[1] catalyze the conversion of diphosphonucleosides such as 3′-phosphoadenosine 5′-phosphate (3′-PAP) into their 5′-monophosphorylated derivatives (5′-AMP). They are ubiquitous among prokaryotes and eukaryotes and belong to a superfamily of Mg^{2+}-dependent, lithium-sensitive phosphohydrolases, which also includes fructose-1,6-bisphosphate 1-phosphatase and various inositol-polyphosphate phosphatases. The prototype of prokaryotic DPNPases is the product of the *Escherichia coli* gene *cysQ*, which, if mutated, abolishes the capacity of bacterial cells to grow on sulfate as the sole source of sulfur (1). The first eukaryotic DPNPase to be isolated was the Li^{+}- and Na^{+}-sensitive enzyme encoded by the *Saccharomyces cerevisiae* gene *HAL2* (2). By preventing the accumulation of 3′-PAP, an inhibitory side product generated upon reduction of 3′-phosphoadenosine 5′-phosphosulfate (3′-PAPS) to sulfite, the Hal2p phosphatase controls the flux of sulfate along the sulfur assimilation pathway (3). Because of the blockage of sulfur assimilation and the concomitant methionine auxotrophy caused by PAP accumulation under conditions of salt-inhibited Hal2p, this enzyme is considered a specific target of salt toxicity (4). During the last few years, various Li^{+}-sensitive phosphatases, all capable of restoring the ability of a yeast *hal2/met22* mutant to grow on sulfate as the sole source of sulfur, have been identified in fungi, plants, and mammals (5–11). Despite the widespread occurrence of PAPS as an activated sulfate derivative for assimilatory sulfate reduction or sulfation reactions, the main metabolic scope of PAP hydrolysis by microbial or higher eukaryotic DPNPases is different. In fact, reductive sulfate assimilation leading to *de novo* cysteine or methionine biosynthesis does not take place in mammals, and it mainly proceeds through a PAPS-independent pathway in plants (12). The major role of DPNPases in these organisms is thus to act in concert with sulfotransferases to drive sulfate ester production through the removal of the inhibitory by-product PAP (13, 14). An even more general role of DPNPases has been revealed by the recent demonstration that PAP accumulation inhibits RNA-processing 5′ → 3′ exoribonucleases (15). This effect is likely due to the fact that 3′-PAP mimics the monomers of a polynucleotide chain, thus preventing phosphodiester bond attack by RNA-processing enzymes. In keeping with this notion, 3′-phosphothymidine 5′-phosphate, the thymine analog of PAP, has been employed previously as a 3′-phosphorylated nucleic acid analog for nucleotidase assays measuring the removal of the 3′-phosphate group by the bifunctional polynucleotide kinase of phage T4 (16). More recently, the same diphosphonucleoside has been utilized as substrate to assay the DNA phosphatase activity of human polynucleotide kinase 3′-phosphatase (PNKP) (17), an enzyme whose ability to dephosphorylate 3′-phosphate termini and to phosphorylate 5′-hydroxyl termini at DNA single strand breaks is predictive of an important function in DNA repair (17, 18).

No DNA 3′-phosphatase activity has thus far been identified in plants, organisms that, besides being subjected to oxidative DNA damage caused by endogenously produced activated oxygen species, are also particularly exposed to (and have a strong capacity to cope with) oxidative agents such as ozone, redox-cycling herbicides, and other environmental pollutants. Based on the assumption that a diphosphonucleoside such as 3′-PAP might be acted upon by both standard DPNPases and DNA 3′-phosphatases, we took advantage of the high sensitivity and lack of sequence bias of *in vivo* functional complementation to

* This work was supported by grants from the National Research Council of Italy, Target Project on "Biotechnology," and the Ministry of University and Scientific and Technological Research (Rome, Italy). The costs of publication of this article were defrayed in part by the payment of page charges. This article must therefore be hereby marked "*advertisement*" in accordance with 18 U.S.C. Section 1734 solely to indicate this fact.

The nucleotide sequence(s) reported in this paper has been submitted to the GenBank™/EBI Data Bank with accession number(s) AF288075 and AF307152.

‡ To whom correspondence should be addressed. Tel.: 39-521-905646; Fax: 39-521-905151; E-mail: s.ottonello@unipr.it.

[1] The abbreviations used are: DPNPases, diphosphonucleoside phosphatases; 3′-PAP, 3′-phosphoadenosine 5′-phosphate; 2′-PAP, 2′-phosphoadenosine 5′-phosphate; 3′-PAPS, 3′-phosphoadenosine 5′-phosphosulfate; PNKP, polynucleotide kinase 3′-phosphatase; bp, base pair(s); MES, 2-(*N*-morpholino)ethanesulfonic acid; tBH, *t*-butyl hydroperoxide; MMS, methyl methanesulfonate; BMS, Black Mexican Sweet.

search for a DNA 3′-phosphatase activity in maize. This approach led to the isolation of ZmDP1 (*Zea mays* diphosphonucleoside phosphatase-1), a new Mg^{2+}-dependent, Li^{+}-sensitive DPNPase, and ZmDP2, the first plant 3′-phosphoesterase thus far identified with the unique ability to catalyze the removal of 3′-phosphate- or 3′-phosphoglycolate-blocking groups from double-stranded DNA molecules and to confer resistance to oxidative DNA damage in a repair-deficient bacterial strain.

EXPERIMENTAL PROCEDURES

Functional Complementation of Bacterial and Yeast DPNPase Mutants—A plasmid-borne (pBluescript KS^{+}, Stratagene) cDNA expression library prepared from the roots of sulfate-deprived maize seedlings (19) was used to search for clones conferring cysteine prototrophy to *E. coli cysQ* mutant cells (strain MC4100, a gift of D. Berg, Washington University Medical School, St. Louis, MO). DNA transformation was carried out by electroporation, and transformants were selected on M9 minimal medium containing 100 μg/ml ampicillin and 0.15 mM isopropyl-β-D-thiogalactopyranoside. Twenty colonies growing in the absence of exogenously supplied cysteine were obtained from the screening of a total of $\sim 10^6$ transformants. Plasmid DNA isolated from such colonies was re-transformed into MC4100 cells and again tested for its ability to confer cysteine prototrophy. Eight clones were thus selected, which, upon restriction analysis and sequence determination, were assigned to two distinct cDNA classes, designated as *ZmDP1* and *ZmDP2*.

For yeast complementation assays, the *ZmDP1* and *ZmDP2* cDNAs were subcloned into the yeast expression vector pFL61 (a gift of M. Minet, CNRS, Gif-sur-Yvette, France). Properly oriented pFL61-*ZmDP* constructs, identified by restriction analysis, were transformed into electrocompetent, *S. cerevisiae met22* mutant cells (strain CD108, kindly provided by Y. Surdin-Kerjan, CNRS). Yeast transformants were first selected for their ability to grow on synthetic dextrose-agar medium supplemented with methionine, but lacking uracil, and subsequently selected on synthetic dextrose medium lacking both uracil and methionine.

DNA and RNA Analyses—Genomic DNA for gel blot analysis was extracted following a previously described procedure (20). DNA samples (20 μg each) were digested with *Eco*RI and *Bam*HI, followed by electrophoresis on a 0.8% agarose gel, which was subsequently denatured and neutralized by standard procedures (21). A random priming labeling kit (Amersham Pharmacia Biotech) was used to prepare ^{32}P-labeled hybridization probes from the *ZmDP1* (1453 bp) and *ZmDP2* (992 bp) cDNAs. Blotting onto Hybond-N nylon membranes (Amersham Pharmacia Biotech), prehybridization, hybridization, and washing were conducted according to the manufacturer's instructions.

Total RNA for RNase protection and primer extension analyses was isolated as described previously (19). ^{32}P-Labeled antisense riboprobes for RNase protection assays were prepared by *in vitro* SP6 RNA polymerase (Promega) transcription of pCRII plasmids (Invitrogen) carrying a 461-bp fragment of *ZmDP1* (positions 675–875) or a 240-bp fragment of *ZmDP2* (positions 109–348), previously digested with either *Pst*I or *Eco*RV, respectively. The resulting riboprobes were 540 nucleotides (*ZmDP1*) and 313 nucleotides (*ZmDP2*) in length, and both included 80 nucleotides of vector-derived sequence. Saturating amounts of a 210-nucleotide maize glyceraldehyde-3-phosphate dehydrogenase (*GAPDH*) riboprobe (including 9 nucleotides of vector-derived sequence) were added to all reactions and used as an internal reference; hybridization (15 μg of total RNA/assay), RNase A/T1 digestion, and sample processing prior to fractionation on denaturing 5% polyacrylamide gels were carried out as described (19). Primer extension analysis was conducted according to a previously described protocol (21). Briefly, a ^{32}P-labeled antisense 28-mer, annealing between positions 79 and 106 of the *ZmDP2* cDNA, was hybridized overnight at 42 °C with 25 μg of total RNA, followed by extension with Moloney murine leukemia virus reverse transcriptase (Superscript II, Life Technologies, Inc.) according to the manufacturer's instructions. Extended products were ethanol-precipitated and analyzed on sequencing gels. The *ZmDP2* cDNA was sequenced in parallel with the same antisense primer, and sequencing reaction products (run on the same gel) were utilized as size markers.

Expression and Purification of Recombinant ZmDP1 and ZmDP2 Proteins—The coding region of *ZmDP1*, starting from position 107 and including 279 bp of 3′-untranslated region plus 20 bp of vector sequence for a total of 1367 bp, was polymerase chain reaction-amplified (25 cycles) using the *ZmDP1* cDNA as template (20 ng), a high-fidelity thermophilic DNA polymerase (Vent, New England Biolabs Inc.), and a pair of primers consisting of a sequence-specific *Nde*I-tailed upstream primer (5′-CCATATGGCTTCGGGGAACC) and the M13 forward/universal primer. The coding region of *ZmDP2*, starting from the methionine codon at position 49 and including 245 bp of 3′-untranslated region plus 20 bp of vector-derived sequence for a total of 965 bp, was similarly amplified using the *ZmDP2* cDNA as template and the sequence-specific *Nde*I-tailed primer 5′-ACCATATGGGGGAGTTTGAAG. The restriction fragments obtained from *Nde*I/*Not*I or *Nde*I digestion of the *ZmDP1* or *ZmDP2* polymerase chain reaction products, respectively, were then ligated into either the *Nde*I/*Not*I sites or the dephosphorylated *Nde*I site of the pET28b expression vector (Novagen) as in-frame fusions with a vector-encoded His_6 tag sequence. After sequence verification, the pET-*ZmDP1* and pET-*ZmDP2* plasmids were electroporated into BL21(DE3) cells (Novagen). Protein expression was induced by adding 1 mM isopropyl-β-D-thiogalactopyranoside and allowed to proceed for 4 h at 30 °C. After cell lysis, recombinant proteins bearing the N-terminal hexahistidine tag were bound to a metal affinity resin (Talon, CLONTECH) equilibrated in 10% glycerol, 300 mM NaCl, and 50 mM sodium phosphate, pH 8.0. After washing with equilibration buffer until the A_{280} of the flow-through was <0.05, bound proteins were eluted with 100 mM imidazole in the same buffer. Protein concentration was determined with the Coomassie Brilliant Blue G-250 dye (Bio-Rad) using bovine serum albumin as a standard. The composition and purity of protein fractions were assessed by gel electrophoresis on SDS-10% polyacrylamide gels (22). Monoclonal antibodies specifically recognizing the N-terminal hexahistidine tag (Amersham Pharmacia Biotech) were utilized for immunoblot analysis of recombinant ZmDP1 and ZmDP2 following the manufacturer's instructions.

Phosphatase Assay—DPNPase activity was measured by quantifying the inorganic phosphate released from various phosphorylated compounds (23). Enzyme assays were conducted at 30 °C for 30 min in 240-μl reaction mixtures containing 0.5 mM magnesium acetate, 200 ng of the purified recombinant proteins, varying concentrations of 3′-PAP, and 50 mM Tris-HCl, pH 8.1, for ZmDP1 or 50 mM MES-KOH, pH 6.1, for ZmDP2. Under these conditions, the activity of both enzymes responded linearly to both protein amount (up to 500 ng) and reaction time (up to 1 h). The kinetic parameters for 3′-PAP hydrolysis were determined by measuring reaction rates at substrate concentrations ranging from 0.01 to 2 mM; nonlinear regression analysis of the data was performed with SigmaPlot (Jandel Scientific). The activities with 2′-PAP, 3′-PAPS, ATP, 3′-AMP, D-*myo*-inositol 1,4-bisphosphate, L-histidinol phosphate, *O*-phospho-L-serine, phosphoglycolic acid, and NADP (all from Sigma) were measured under conditions of optimal activity for each enzyme at a fixed substrate concentration (0.1 mM).

DNA 3′-Phosphoesterase Assays—Radioactive ^{32}P labeling of the 5′-OH/21-mer/3′-P (21p) and 5′-OH/21-mer/3′-OH oligonucleotides (MWG Biotech) was carried out as described previously (24), but with a labeling reaction time of only 30 s at 37 °C. Annealing reactions for the preparation of the 1-nucleotide gapped p21p·23/45-mer duplex were carried out at 70 °C for 5 min in the presence of a 2-fold molar excess of the 23-mer and 45-mer oligonucleotides with respect to the labeled p21p oligonucleotide, followed by cooling to room temperature over a period of 2 h. Full oligonucleotide annealing was verified by nondenaturing polyacrylamide gel electrophoresis. Unless otherwise specified, DNA 3′-phosphatase assays were conducted at 37 °C for 7 min in 15-μl reaction mixtures containing 50 mM Tris-HCl, pH 7.0, 10 mM $MgCl_2$, 1 mM dithiothreitol, 0.035–0.15 μM oligonucleotide substrate, and 1 ng of purified ZmDP1 or ZmDP2. Reactions were stopped by adding 7.5 μl of denaturing loading dye solution; reaction products were fractionated on 7 M urea and 8% polyacrylamide sequencing gels, which were subsequently subjected to phosphorimage analysis (see below). The kinetic parameters for p21p 3′-dephosphorylation by ZmDP2 were determined by measuring reaction rates at p21p concentrations ranging from 1 to 160 μM in the presence of a fixed amount (4 ng) of ZmDP2; nonlinear regression analysis of PhosphorImager data was performed with SigmaPlot. A similar assay run under identical experimental conditions was used to analyze the 3′-phosphodiesterase activity of ZmDP2. A double-stranded DNA substrate containing a 3′-terminal phosphoglycolate group was prepared by bleomycin/iron(II) cleavage of a synthetic oligonucleotide duplex as described previously (25).

Gradient Plate DNA Repair Assays—The repair-deficient double mutant *xth,nfo* BW528 strain and the isogenic wild-type *E. coli* strain BW32 (a gift of B. Weiss, Emory University, Atlanta, GA) were transformed with the empty pBluescript vector, pBluescript-ZmDP1, pBluescript-ZmDP2, or the positive control plasmid pNfo (a pBluescript derivative carrying the *E. coli* endonuclease IV gene, kindly provided by D. Ramotar, Hopital Maisonneuve-Rosemont, Montreal, Canada). All the above transformants were used for DNA damage resistance assays

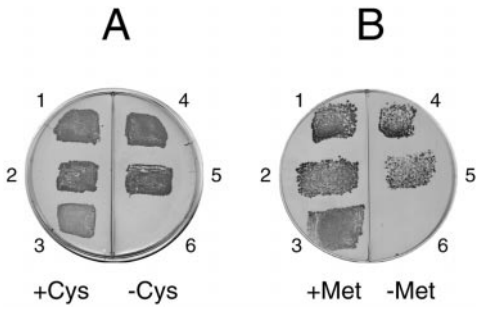

FIG. 1. **Functional complementation of microbial DPNPase mutant strains by the *ZmDP1* and *ZmDP2* cDNAs.** *A*, bacterial *cysQ* mutant cells were transformed with expression vector constructs carrying the *ZmDP1* cDNA (*patches 1* and *4*), the *ZmDP2* cDNA (*patches 2* and *5*), or neither (*patches 3* and *6*) and plated onto minimal M9 medium with (+*Cys*) or without (−*Cys*) cysteine. *B*, yeast *hal2/met22* mutant cells were transformed as described for *A* (see "Experimental Procedures" for expression vector details) and plated onto minimal synthetic dextrose medium with (+*Met*) or without (−*Met*) methionine.

(26), which were conducted on LB-ampicillin-agar plates with linear concentration gradients of H_2O_2, tBH, or MMS.

Other Methods—Seed sterilization, germination, and hydroponic culture of 15-day-old seedlings of the maize hybrid Paolo (Dekalb, Chiarano, Italy) were carried out as described (19). Black Mexican Sweet cells (kindly provided by S. Lobreaux, CNRS, Montpellier, France) were maintained and propagated as described (27). *E. coli* XL1-Blue cells (Stratagene) were used for plasmid propagation. DNA sequencing was performed with the dideoxy chain termination method using the Thermo-Sequenase cycle sequencing kit (Amersham Pharmacia Biotech). Phosphorimages of dried gels and filters were obtained with a Personal Imager FX (Bio-Rad) and analyzed using Multi-Analyst/PC software (Bio-Rad). Sequence similarity searches were conducted against the NCBI Non-redundant Protein Sequence Database. Multiple alignments were constructed with the ITERALIGN Version 1.1 program set to recognize alignment blocks including all the sequences under examination (28). Polynucleotide kinase assays were conducted at 37 °C for 30 min in 10-μl reaction mixtures containing 50 mM Tris-HCl, pH 7.0, 1 μCi of [γ-^{32}P]ATP (Amersham Pharmacia Biotech; 5000 Ci/mmol), 10 pmol of the 5′-OH/23-mer oligonucleotide (see above), plus either 10 ng of purified ZmDP2 or 3 units of phosphatase-free T4 polynucleotide kinase (Roche Molecular Biochemicals) utilized as a control.

RESULTS

Isolation of Two Distinct Maize cDNAs Functionally Complementing Bacterial and Yeast DPNPase Mutants—A plasmid-borne maize cDNA library was transferred into *E. coli* DPNPase *cysQ* mutant cells, which are cysteine auxotrophs, and transformants were selected on the basis of their ability to grow on synthetic medium containing sulfate as the sole source of sulfur. Following the initial isolation of cysteine prototroph colonies and a second round of selection, plasmid DNA was isolated from individual colonies and analyzed by restriction digestion. Two different cDNA inserts, *ZmDP1* (1453 bp) and *ZmDP2* (992 bp), were identified. As shown in Fig. 1*A*, when reintroduced into *cysQ* mutant cells, both cDNAs were capable of supporting bacterial growth on cysteine-free synthetic medium. Sequence analysis of the *ZmDP1* cDNA revealed a coding region corresponding to a polypeptide of 355 amino acids, very closely related throughout its entire sequence to previously identified plant DPNPases and sharing maximum similarity (82%) and identity (76%) with the rice RHL phosphatase (5). Instead, the 248-amino acid-long polypeptide encoded by the *ZmDP2* cDNA did not share any sequence similarity with known DPNPases. This was quite surprising and in apparent contrast with the seemingly equal capacity of the *ZmDP1* and *ZmDP2* cDNAs to complement the *cysQ* mutation. To exclude the possibility that *ZmDP2* complementation might result from some kind of indirect, host-related effect (*e.g.* the stabilization or activation of a bacterial phosphatase other than CysQ)

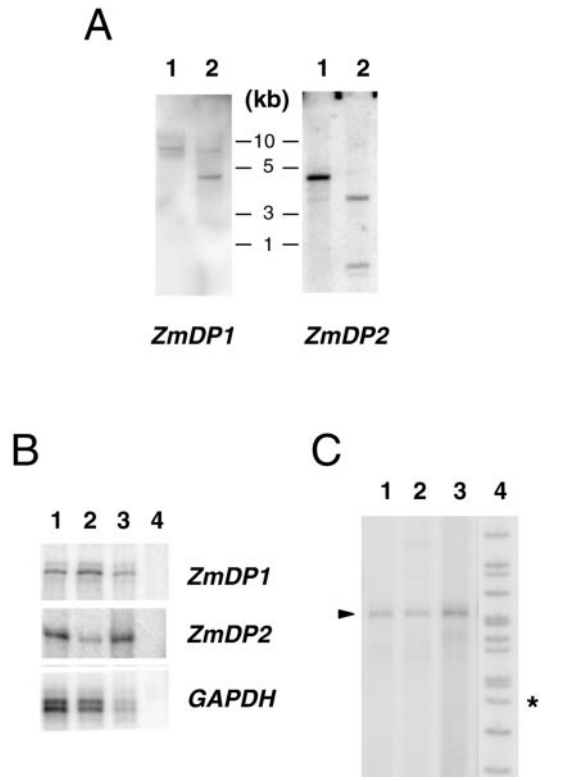

FIG. 2. **DNA gel blot and RNA expression analyses of *ZmDP1* and *ZmDP2*.** *A*, DNA gel blot analysis. Maize genomic DNA (20 μg/lane) digested with *Eco*RI (*lanes 1*) or *Bam*HI (*lanes 2*) was probed with either the *ZmDP1* (1453 bp) or *ZmDP2* (992 bp) cDNA. The sizes of DNA length markers run on the same gel are indicated in kilobase pairs (*kb*). *B*, RNase protection analysis. Total RNA samples derived from maize roots (*lane 1*), maize shoots (*lane 2*), maize BMS suspension culture cells (*lane 3*), or a control yeast RNA (*lane 4*) were analyzed using antisense *ZmDP1* and *ZmDP2* riboprobes as indicated on the right. A maize glyceraldehyde-3-phosphate dehydrogenase (*GAPDH*) antisense riboprobe was included in all hybridization reactions as an internal standard. *C*, primer extension analysis of the *ZmDP2* mRNA. Total RNA samples extracted from roots (*lane 1*), shoots (*lane 2*), or BMS cells (*lane 3*) were subjected to primer extension analysis using a ^{32}P-labeled antisense oligonucleotide annealing between positions 79 and 106 of the *ZmDP2* cDNA. The *arrowhead* indicates the main extension product. Shown in *lane 4* are the products of an A-track chain termination sequencing reaction conducted in parallel with the same antisense oligonucleotide utilized for primer extension. The position corresponding to the first nucleotide of the *ZmDP2* cDNA is indicated with an *asterisk*.

rather than from true functional replacement, the two maize cDNAs were inserted into a multicopy yeast expression vector and tested for their ability to restore methionine prototrophy in an *S. cerevisiae* DPNPase *hal2/met22* mutant (2, 29). The data presented in Fig. 1*B* show that *ZmDP2* is indistinguishable from *ZmDP1* in its ability to complement the methionine auxotrophy of the yeast *hal2/met22* mutant, thus confirming its *bona fide* identification as a novel plant phosphatase functionally equivalent to, yet structurally distinct from, previously known DPNPases.

DNA Gel Blot and Expression Analysis of ZmDP1 and ZmDP2—Maize genomic DNA digested with restriction enzymes *Eco*RI and *Bam*HI, which do not cut within the *ZmDP1* and *ZmDP2* cDNAs, was utilized for DNA gel blot analysis. As shown in Fig. 2*A* (*lanes 1*), a single hybridizing band was recognized by either cDNA probe when using *Eco*RI-digested DNA. Similarly, a single band pattern for *ZmDP1* and one predominant *ZmDP2* hybridizing band, with an additional smaller band probably due to an intronic cleavage site, were revealed by DNA gel blot analysis of *Bam*HI-digested genomic DNA (Fig. 2*A*, *lanes 2*). This indicates that single copies of

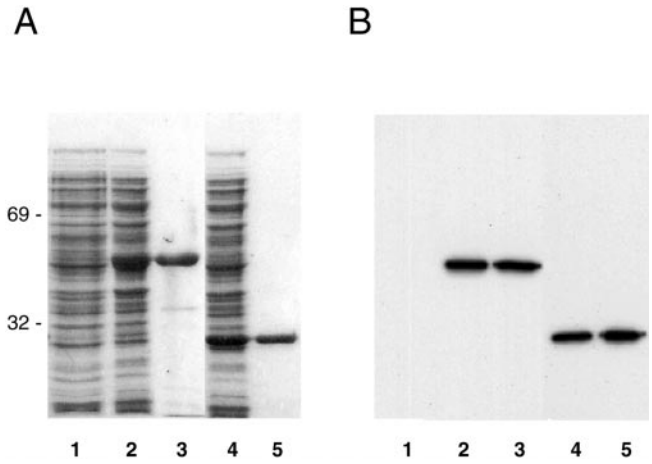

FIG. 3. **Expression and purification of recombinant ZmDP1 and ZmDP2.** *A*, Coomassie Blue-stained SDS-10% polyacrylamide gel of total lysates derived from isopropyl-β-D-thiogalactopyranoside-induced bacterial cells (BL21(DE3)) transformed with the empty pET28b vector (*lane 1*), the pET-*ZmDP1* plasmid (*lane 2*), or the pET-*ZmDP2* plasmid (*lane 4*). Highly purified fractions (0.5 μg) of histidine-tagged recombinant proteins generated by metal affinity chromatography of either the ZmDP1 or ZmDP2 soluble lysate are shown in *lanes 3* and *5*, respectively. The migration positions of molecular mass markers (in kilodaltons) run on the same gel are indicated on the left. *B*, immunoblot analysis of the protein samples shown in *A*. A monoclonal antibody specifically recognizing the N-terminal hexahistidine tag was utilized for immunodetection. The loading order and electrophoresis conditions are the same as described for *A*.

ZmDP1 and *ZmDP2* are present in the maize genome. As further shown by the RNase protection data reported in Fig. 2*B*, transcripts recognized by antisense RNAs derived from both cDNAs accumulated in the roots and shoots of 15-day-old seedlings as well as in cultured maize Black Mexican Sweet (BMS) cells. The *ZmDP1* RNA was expressed at comparable levels in the two tissues and in BMS cells, whereas a higher accumulation of the *ZmDP2* messenger was detected in roots and in cultured cells (4- and 6-fold, respectively) compared with shoots.

No informative N-terminal sequence homology to DPNPases or other known proteins (see below) and no significant similarity to translational initiation consensus sequences were detected in the case of the *ZmDP2* open reading frame. A primer extension analysis was thus conducted to map the 5′-end of the *ZmDP2* mRNA. As revealed by the data reported in Fig. 2*C*, a predominant extended product, corresponding to an mRNA only 18 nucleotides longer than the cDNA isolated by functional complementation, was detected in maize BMS cells and tissues.

Functional Characterization of the ZmDP1 and ZmDP2 Phosphatases—To gain insight into the enzyme activity of the two ZmDP phosphatases, both proteins were expressed in *E. coli* and comparatively analyzed for their ability to catalyze the dephosphorylation of various phosphorylated compounds and for their sensitivity to cation inhibition. To achieve high-level protein expression and easy purification, the two *ZmDP* cDNAs (starting from the consensus initiator methionine codon of *ZmDP1* and from the first methionine encoded by the *ZmDP2* cDNA) were inserted into the expression plasmid pET28 as in-frame fusions with a vector sequence coding for a 20-amino acid N-terminal extension, including a metal-binding hexahistidine tag. As shown in Fig. 3, polypeptides of the expected molecular masses (40 and 28 kDa for histidine-tagged ZmDP1 and ZmDP2, respectively), recognized by an anti-His_6 monoclonal antibody, became detectable upon isopropyl-β-D-thiogalactopyranoside induction (*A* and *B*, *cf. lanes 1* with *lanes 2* and *4*) and were purified to near-homogeneity by metal affinity chromatography (*A* and *B*, *lanes 3* and *5*). Recombinant ZmDP phosphatases were initially tested for their ability to release inorganic phosphate from 3′-PAP. As shown in Table I, ZmDP1 and ZmDP2 both catalyzed the Mg^{2+}-dependent dephosphorylation of this diphosphonucleoside: the apparent K_m for 3′-PAP hydrolysis by ZmDP1 was ~4-fold lower than the corresponding value measured for ZmDP2, but dephosphorylation reactions supported by either enzyme were characterized by similar apparent V_{max} values. Using 3′-PAP as a reference substrate, we next investigated the ability of the two maize phosphatases to utilize other phosphorylated compounds as substrates. As further shown in Table I, where the activity toward 3′-PAP was arbitrarily set to 100%, ZmDP1 catalyzed the dephosphorylation of 2′-PAP and 3′-PAPS with nearly the same efficiency as that determined for 3′-PAP and also utilized inositol 1,4-bisphosphate as substrate, albeit with an ~10-fold reduced efficiency. In contrast, 2′-PAP was an extremely poor substrate for ZmDP2, and the only other bisphosphate besides 3′-PAP that was efficiently dephosphorylated by this enzyme was 3′-PAPS. Furthermore, as documented by the IC_{50} values reported in Table II, 3′-PAP dephosphorylation by ZmDP2 was ~12-fold less sensitive to Li^+ inhibition than the same reaction catalyzed by ZmDP1. Both enzymes were not inhibited by physiological Na^+ and K^+ ion concentrations, whereas Ca^{2+} was a more effective Mg^{2+}-competitive inhibitor of the ZmDP2 than the ZmDP1 enzyme.

ZmDP2 Is a DNA 3′-Phosphatase Acting on the 3′-Phosphorylated Termini of DNA Single Strand Breaks—A distinguishing feature of the ZmDP2 phosphatase, besides its lower lithium sensitivity, was its marked discrimination against 2′-PAP, the highest thus far reported for any DPNPase. Such strong selectivity for 3′-phosphorylated substrates is reminiscent of the position-specific attack of mononucleotides and oligonucleotides by certain nucleotidases, thus suggesting a possible relationship between ZmDP2 and enzymes acting on nucleic acids. This hypothesis was experimentally verified by assaying the activity of recombinant ZmDP2 on oligonucleotide substrates (schematically represented in Fig. 4*A*) previously utilized for mammalian PNKPs (24). As shown in Fig. 4*B*, which compares the output of dephosphorylation reactions conducted in the presence of a fixed concentration of the 1-nucleotide gapped p21p·23/45-mer duplex (indicated as *Substrate* in Fig. 4*A*) and increasing amounts of either ZmDP1 (*lanes 5–8*) or ZmDP2 (*lanes 1–4*), only the latter enzyme catalyzed the nearly complete conversion of the p21p oligonucleotide into a more slowly migrating species, whose electrophoretic mobility was the same as that of the 5′-^{32}P-labeled p21 3′-hydroxyl oligonucleotide indicated as *Product* in Fig. 4*A*. This demonstrates that ZmDP2, but not ZmDP1, acts as a DNA 3′-phosphatase that catalyzes the removal of 3′-phosphate-blocking groups from DNA strand breaks. Moreover, the fact that both proteins were expressed in the same bacterial strain and purified with an identical affinity chromatography procedure rules out the possibility that the DNA 3′-phosphatase activity exhibited by recombinant ZmDP2 is actually due to a contaminating bacterial enzyme.

Single-stranded and gapped double-stranded 3′-phosphate termini were both efficiently dephosphorylated by ZmDP2 (data not shown), and the apparent K_m and V_{max} values for single-stranded p21p dephosphorylation were 12 ± 3 μM and 56 ± 4 μmol of product/h/mg of protein, respectively. Similar to PAP hydrolysis, DNA dephosphorylation by ZmDP2 was strictly Mg^{2+}-dependent and, as shown in Fig. 5, was largely insensitive to Li^+, Na^+, and K^+ inhibition. Interestingly, however, the DNA 3′-phosphatase activity of ZmDP2 was strongly inhibited by both Cd^{2+} and Cu^{2+} (but not by Ni^{2+}), with half-

TABLE I

Substrate specificity and kinetic parameters of ZmDP1 and ZmDP2

The activity measured with different phosphorylated compounds (each at a concentration of 0.1 mM) is expressed as the percentage of the activity with 3′-PAP. Kinetic parameters were determined as described under "Experimental Procedures." The results are the average of triplicate determinations that differed by <10% of the mean.

Substrates	ZmDP1	K_m	V_{max} [a]	ZmDP2	K_m	V_{max} [a]
		μM			μM	
3′-PAP	100	33	72	100	126	66
3′-PAPS[b]	82			67		
2′-PAP	100			6		
3′-AMP	<1			<1		
ATP	<1			<1		
NADP	<1			<1		
Inositol 1,4-bisphosphate	13			<1		
O-Phospho-L-serine	<1			<1		
Phosphoglycolic acid	<1			<1		
L-Histidinol phosphate	<1			<1		

[a] V_{max} values are given as micromoles of released inorganic phosphate/h/mg of protein.

[b] The presence of lithium ions (4 mol of Li^+/mol of PAPS) in commercial preparations of 3′-PAPS (Sigma) was taken into account by assaying the reference substrate 3′-PAP in parallel reactions containing the same concentration of Li^+ (0.4 mM) as that provided by 3′-PAPS.

TABLE II

Effect of different cations on the PAP phosphatase activity of ZmDP1 and ZmDP2

Results are expressed as IC_{50} (mM) values, *i.e.* the cation concentration that caused 50% inhibition of phosphatase activity relative to a reference reaction containing only the Mg^{2+} cation. A maximum cation concentration of 500 mM was tested; all cations were supplied as chloride salts to standard reaction mixtures containing 0.1 mM 3′-PAP and 200 ng of recombinant enzymes.

Cation	ZmDP1	ZmDP2
Li^+	1.6	20
Na^+	Not sensitive	160
K^+	Not sensitive	140
Ca^{2+}	0.35	0.09

inhibitory concentrations of 67 and 40 μM, respectively (Fig. 5).

ZmDP2 Rescues DNA Damage Sensitivity in a DNA Repair-deficient E. coli Strain—DNA strand breaks with 3′-blocked termini are produced by nucleases such as DNase II as well as by various oxidative DNA-damaging agents (30). The prototypes of 3′-phosphoesterases involved in the repair of such lesions are *E. coli* exonuclease III and endonuclease IV, which catalyze the removal of a variety of 3′-blocking groups, including the 3′-phosphate and 3′-phosphoglycolate groups generated by the chemical oxidants hydrogen peroxide and *t*-butyl hydroperoxide (26, 31, 32). Accordingly, *E. coli* strains lacking both exonuclease III (*xth*) and endonuclease IV (*nfo*) display a marked hypersensitivity to various oxidative DNA-damaging agents. To find out whether the newly identified plant DNA 3′-phosphatase activity may indeed play a role in DNA repair, we tested its ability to confer DNA damage resistance to the double mutant *xth,nfo* BW528 strain (26). Besides *ZmDP2*, the *ZmDP1* cDNA and a plasmid actively expressing bacterial endonuclease IV (pNfo, used as positive control) were transformed into both the double mutant BW528 strain and the isogenic wild-type BW32 strain. A gradient plate assay, in which mutant cells grow only a short distance into a gradient of increasing genotoxic agent concentration compared with repair-proficient wild-type cells, was used for these experiments. As shown in Fig. 6, ZmDP2 and endonuclease IV (Nfo), but not ZmDP1, conferred to strain BW528 resistance against the DNA-damaging agents H_2O_2 (*A*), tBH (*B*), and MMS (*C*). Hydrogen peroxide sensitivity was fully rescued by ZmDP2, whereas only a partial, yet highly significant rescue was observed in the case of tBH. Chemically different 3′-blocked termini with either a terminal phosphate or phosphoglycolate group are the main products of H_2O_2 and tBH attack, respectively (33). Using a partially double-stranded DNA with a 3′-terminal phosphoglycolate group as substrate and assay conditions similar to those previously employed for the DNA 3′-phosphatase activity, we thus directly tested the ability of ZmDP2 to also act as a 3′-phosphodiesterase. As shown by the results presented in Fig. 7, this appears to be the case. In fact, increasing amounts of a lower mobility species, comigrating with the unblocked control oligonucleotide BL1–17, accumulated in reaction mixtures containing the 3′-phosphoglycolate-blocked substrate BL1–17PG/BL2 and increasing amounts of ZmDP2.

Features of the Deduced ZmDP2 Protein Sequence—When used as a query for a similarity search, the deduced ZmDP2 protein sequence led to the identification of partially similar amino acid sequences from various organisms (Fig. 8). All of these sequences are from predicted proteins of unknown function, with the sole exception of PNKP, a sequence coding for a recently identified human polynucleotide kinase 3′-phosphatase that is thought to be involved in DNA repair (17, 18). The regions of similarity between ZmDP2 and PNKP include two conserved amino acid blocks (*underlined* in Fig. 8) resembling sequence motifs recently identified in a superfamily of phosphohydrolases as distinct domains separated by a consensus distance of 102–191 amino acids (34). Interestingly, a C-terminal polypeptide extension (not shown in Fig. 8) containing a typical kinase motif is present in human PNKP (17, 18) and in all of the other non-plant sequences, but is missing in ZmDP2 as well as in the *Arabidopsis* polypeptide. This suggests that at variance with PNKP, ZmDP2 may be endowed only with DNA 3′-phosphatase activity. Accordingly, no ATP-dependent kinase activity was detected in ZmDP2-supplemented reaction mixtures containing the 5′-OH/23-mer oligonucleotide reported in Fig. 4*A* (data not shown).

DISCUSSION

Two novel, structurally and functionally distinct maize phosphatases have been identified on the basis of their ability to alleviate PAP accumulation, and thus cysteine auxotrophy, in an *E. coli* DPNPase *cysQ* mutant strain. The first of them, ZmDP1, displays all the hallmarks of previously described, Mg^{2+}-dependent, Li^+-sensitive DPNPases. It shares the highest sequence similarity with the rice RHL enzyme (5), the only other known DPNPase from monocotyledons; but its sodium insensitivity and ability to utilize inositol 1,4-bisphosphate as substrate (albeit with a reduced efficiency compared with PAP) suggest that it is more related functionally to the SAL2 DPNPase from *Arabidopsis* (6). As predicted by its isolation as a *cysQ*-complementing activity, the other phosphatase, ZmDP2, also efficiently dephosphorylates 3′-PAP (with a similar V_{max} and an ~4-fold higher K_m compared with ZmDP1), but strongly

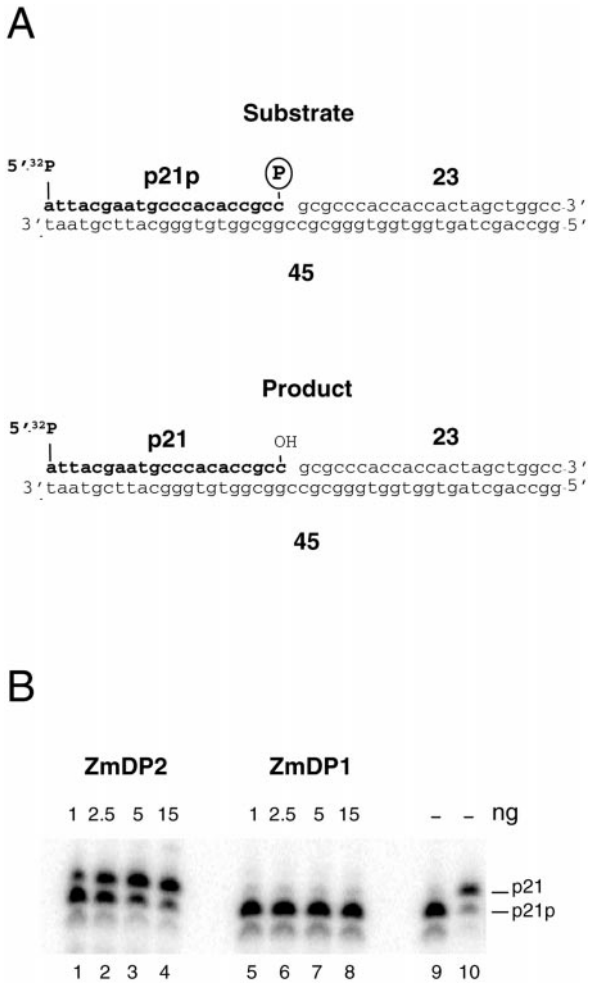

FIG. 4. **DNA 3′-phosphatase activity of ZmDP2.** *A*, schematic representation of the oligonucleotides and model substrates utilized for DNA 3′-phosphatase assays. The double-stranded DNA shown at the top (*Substrate*) was prepared by annealing three oligonucleotides (5′-^{32}P-labeled p21p, 23-mer, and 45-mer) to generate a 1-nucleotide gap with a 3′-phosphate terminus. The duplex generated by 3′-phosphate hydrolysis of the substrate DNA is shown below (*Product*). p21p and p21 refer to the 21-mer oligonucleotides with both 3′- and 5′-phosphorylated termini or only 5′-phosphorylated termini, respectively. The termini relevant to this study are indicated above the oligonucleotide sequences; the 3′-phosphate group undergoing hydrolysis is *circled*. The 5′-phosphate of both p21p and p21 was radiolabeled. *B*, phosphorimage of a 7 M urea and 8% polyacrylamide gel showing the denatured, single-stranded substrate (p21p) and product (p21) of DNA 3′-dephosphorylation reactions conducted with the gapped duplex reported in *A* (35 nM) in the presence of the indicated amounts of either ZmDP2 (*lanes 1–4*) or ZmDP1 (*lanes 5–8*). Unreacted, 5′-labeled p21p (*lane 9*) and p21 (*lane 10*) were run alongside as standards; their migration positions are indicated on the right.

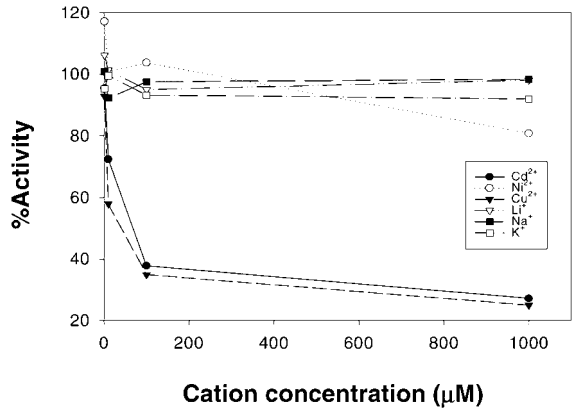

FIG. 5. **Effect of different cations on the DNA 3′-phosphatase activity of ZmDP2.** The p21p oligonucleotide (0.15 μM) was incubated with recombinant ZmDP2 (1 ng) in the presence of increasing concentrations of $CdCl_2$ (●), $NiSO_4$ (○), $CuCl_2$ (▼), LiCl (▽), NaCl (■), or KCl (□). Reaction conditions were as described under "Experimental Procedures," except for the omission of dithiothreitol. The results are expressed as percentages of the activity measured in the absence of any added salt and are the average of at least two independent experiments, performed in duplicate, that differed by <10% of the mean.

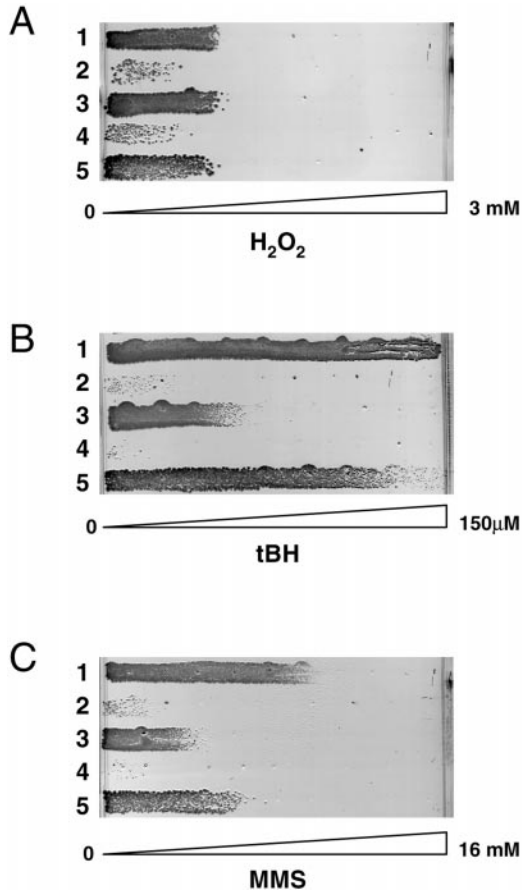

FIG. 6. **Resistance to DNA-damaging agents conferred by ZmDP2 in a repair-deficient *E. coli* strain.** Wild-type *xth*$^+$*nfo*$^+$ BW32 cells harboring the empty pBluescript vector (*rows 1*) or double mutant *xth,nfo* BW528 cells harboring the empty pBluescript (*rows 2*), pBluescript-ZmDP2 (*rows 3*), pBluescript-ZmDP1 (*rows 4*), or pNfo (*rows 5*) plasmid were grown on LB-ampicillin-agar plates with the indicated linear gradients of H_2O_2 (*A*), tBH (*B*), and MMS (*C*).

discriminates against 2′-PAP and is much less sensitive to lithium inhibition. The most remarkable feature of ZmDP2 is, however, its unique ability to dephosphorylate 3′-phosphate-blocked single-stranded or gapped double-stranded DNA with an apparent K_m ~10-fold lower than that determined for 3′-PAP. Despite its more favorable K_m value, the dephosphorylation of DNA 3′-phosphate termini might, in principle, be viewed as a side activity of ZmDP2. Two distinct lines of evidence strongly argue against this possibility, however. The first is the complete sequence divergence between ZmDP2 and classical DPNPases, as opposed to its partial sequence similarity to human PNKP, an enzyme likely to be involved in DNA repair (17, 18). The second, more direct evidence is the capacity of ZmDP2, but not ZmDP1, to restore wild-type resistance to hydrogen peroxide damage in DNA repair-deficient *E. coli* cells to the same extent as the bacterial repair enzyme endonuclease IV. Hydrogen peroxide is known to preferentially induce the formation of DNA strand breaks with 3′-phosphate termini (30, 33). This finding thus provides an important *in vivo* validation of the DNA 3′-phosphatase activity of ZmDP2, initially re-

vealed by *in vitro* assays conducted on a gapped double-stranded DNA substrate.

Besides the complete rescue of DNA damage sensitivity observed with H_2O_2, ZmDP2 also conferred protection against tBH (Fig. 6). Single strand breaks with 3′-phosphoglycolate-blocked termini are the main products of tBH attack (33). These are not typical substrates of 3′-phosphatase action, yet all the 3′-repair enzymes thus far identified catalyze the hydrolysis of both 3′-phosphate and 3′-phosphoglycolate groups, often with different specific activity ratios (25, 30). Moreover, in the case of the *Drosophila* repair enzyme RRP1, mutagenesis studies have shown that both 3′-phosphoesterase activities are associated with the same active site (33). In keeping with the above data, we found that ZmDP2 is also endowed with both 3′-repair activities, albeit with a preference for 3′-phosphate-blocked termini.

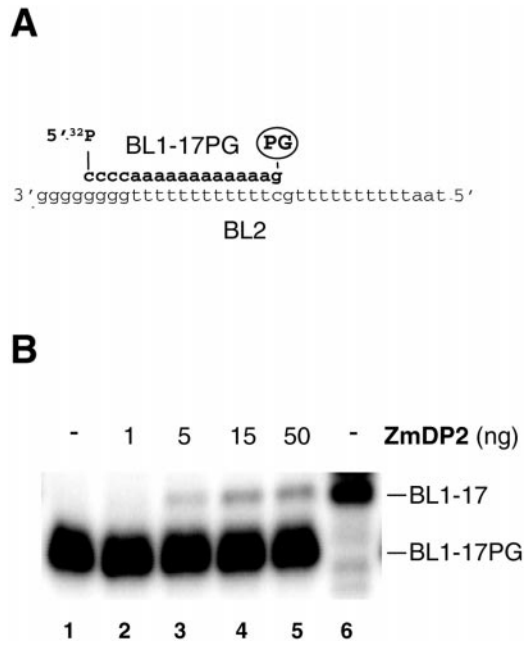

FIG. 7. **DNA 3′-phosphodiesterase activity of ZmDP2.** *A*, schematic representation of the oligonucleotide substrate utilized for DNA 3′-phosphodiesterase assays. The partially double-stranded 3′-phosphoglycolate substrate BL1–17PG/BL2 was prepared using a previously described procedure (25); the 3′-phosphoglycolate (*PG*) group undergoing hydrolysis is *circled*. An oligonucleotide identical to BL1–17PG, but lacking the 3′-phosphoglycolate group, referred to as BL1–17, was used as a gel migration control of the 3′-phosphoglycolate hydrolysis product. The 5′-phosphates of both BL1–17PG and BL1–17 were radiolabeled. *B*, phosphorimage of a 7 M urea and 16% polyacrylamide gel showing the unconverted denatured BL1–17PG substrate and the BL1–17 product that accumulated in reaction mixtures containing a fixed concentration of BL1–17PG/BL2 (10 nM) and the indicated amounts of ZmDP2. Unreacted, 5′-labeled BL1–17PG (*lane 1*) and BL1–17 (*lane 6*) were run alongside as standards; their migration positions are indicated on the right.

Similar to human PNKP (17), ZmDP2 also conferred partial protection against the alkylating agent MMS, whose main DNA damage products are abasic (apurinic/apyrimidinic) sites. This may reflect an intrinsic apurinic/apyrimidinic endonuclease activity, as reported previously for other multifunctional repair enzymes such as the endonuclease/phosphoesterase encoded by the bacterial gene *nfo* (30, 32, 35) and the apurinic endonuclease redox protein ARP from *Arabidopsis* (36). Alternatively, the partial protection against MMS can result from an indirect effect whereby bacterial apurinic/apyrimidinic site-processing enzymes other than endonuclease IV and exonuclease III (*e.g.* formamidopyrimidine-DNA glycosylase, endonuclease III, or endonuclease VIII) convert MMS-generated apurinic/apyrimidinic sites into 3′-phosphate single strand breaks that are subsequently acted upon by ZmDP2.

Altogether, the present data delineate ZmDP2 as the first plant enzyme capable of converting 3′-blocked DNA termini, generated by oxidative damage, into priming sites competent for reparative DNA polymerization. Based on sequence homology, a similar role in DNA repair can also be attributed to the previously uncharacterized protein encoded by the conceptually assembled *Arabidopsis* DNA sequence (37) that scored highest in our BLAST searches.

Similar to ZmDP2, most of the eukaryotic DNA repair enzymes thus far identified are constitutively and ubiquitously expressed even in the absence of genotoxic agent exposure (30). This likely reflects the involvement of such enzymes not only in the response to acute genotoxicity, but also in the housekeeping defense against DNA damage caused by oxygen radicals, which are normal by-products of aerobic metabolism in all organisms. Oxygen radicals, the actual causative agents of much oxidative DNA damage, can also be generated upon reaction of reduced transition metals with H_2O_2, a key mediator of the hypersensitive response triggered by plant-pathogen interaction. In ad-

```
Z.mays          :       mgefeegaeknleeaklpagnkmigpsisfslsdikkeyknatlpahwkvfdtvIFREKEDGLHASSKIAAFDFDGCLANTSMKRV :  86
A.thaliana      : eedesltkakqqmakthkvnmsestsqveveaeitlsasdvkdkyrdanllpkwkafetvIFLERDDGLNDSEKIAAFDFDGCLAKT.SVKI : 618
S.pombe         :      msskkrkspppqesltsyfeksskskkygsqnkdsdssstclqqkieiqwsitdsLYLAKYGKLKKTKKFIAFDLDGTLIKTKSGRV :  87
D.melanogaster : qngerelkhgdlveivygrhqfevvfnpppeydkekaeplsttlspsekserwdssgngkLVIFTSVGVKGSEKIAGYDMDGTLIKTKSGLV : 181
H.sapiens       : lylvnglhpltlrweetrtpesqpdtppgtplvsqdekrdaelpkkrmrksnpgwenlekLLVFTAAGVKPQCKVAGFDLDGTLITTRSGKV : 184

Z.mays          : ...GADQWSLQHKSIPEKLQRLYDDGYKLVIFTNESNIERWKnkrqqavdskvgRLDNFIECVKAPIQVFIACglgkgkgip..DDPYRKPN : 173
A.thaliana      : v..GADAWSLMYPSIEEKLQSLHDQGYKLVIFTNESNIDRWKnkrqaavdskigRLNSFIERVKVPIQVFIACgvsssggkggkDDLYRKPK : 697
S.pombe         : fskDAADWTWWHPSVVPKLKALYQDNYSLVIFSNQNGIPR.Kpsaghtfqm...KIRAIFESLDLPIVLYAAIl.....KDKFRKPL : 165
D.melanogaster : fpkNTDDWQTIFPEVEEKLKNLHKDGFKICLFTNQGGIARGKinlddfkv....KIKHIVAKLGVPIQVFIAIg.....DGFYRKPL : 259
H.sapiens       : fptGPSDWRILYPEIPRKLRPLEAEGYKLVIFTNQMSIGRGKlpaeefka....KVEAVVEKLGVPFQVLVATh.....AGLYRKPV : 262

Z.mays          : PGMWWLMAQHFNSGIKIDM.DQsfYVGDAAGR.....ENDHSDADIEFAKAIGLKFHVPEEYFgf                  : 232
A.thaliana      : AGMWQLMKKHFNSGIAIDM.DKsfYVGDAAGR.....KMDHSDADIKFAQASGLKFFTPEEYFipsstspgt           : 774
S.pombe         : TGMWNSFLKDVNRSIDLSF.IK..YVGDAAGR.....PGDHNSTDLKFAENIGIKFETPEQFFlghsfvppnfesfhpkny : 238 (421)
D.melanogaster : TGMWQHLKSEMNDGVPIQE.DRcfPVGDAAGRpetgkgatkrRKDHSLVDRLFAANVGISFYTPEVHFLgkqveqwnkpdfeptsv : 344 (521)
H.sapiens       : TGMWDHLQEQANDGTPISIgDSi.FVGDAAGRpanwapgrk.KKDFSCADRLFALNLGLPFATPEEFFLkwpaagfelpafdprtv : 352 (521)
```

FIG. 8. **Alignment of ZmDP2 with polypeptide sequences from other organisms.** The polypeptide sequence of ZmDP2 was aligned with the four best scoring sequences identified by the BLAST algorithm: uncharacterized sequences from *Arabidopsis thaliana* (NCBI accession number BAA97052 (37); 61% identity and 72% similarity), *Schizosaccharomyces pombe* (NCBI accession number O13911; 27% identity and 44% similarity), *Drosophila melanogaster* (NCBI accession number AAF54229; 27% identity and 41% similarity), and human PNKP (NCBI accession number AAD50639 (17, 18); 28% identity and 43% similarity). Amino acid residues that are conserved in at least four of the five sequences are *boxed*; *uppercase letters* indicate amino acid blocks that are alignable in all five sequences (28). Gaps introduced to optimize the alignment are indicated by *dots*; sequences resembling consensus phosphohydrolase motifs (34) are *underlined*.

dition, because of their lifestyle, plants are particularly exposed not only to oxygen radical-generating pollutants such as ozone and redox-cycling herbicides, but also to other compounds (*e.g.* heavy metals) that, by inhibiting defense enzyme activities, may indirectly increase oxygen radical accumulation and/or drastically impair DNA damage repair. In the case of ZmDP2, this kind of interference is well exemplified by the results of metal inhibition experiments, which showed half-inhibition of DNA 3′-phosphate hydrolysis by micromolar Cd^{2+} and Cu^{2+} concentrations, and by the potential, competitive inhibition of ZmDP2 DNA 3′-phosphoesterase activity by the high levels of 3′-PAP that may accumulate under conditions of strong and persistent Li^{+} exposure, resulting in the inhibition of the DPNPase activity of ZmDP1.

Given the complexity and chemical diversity of oxidative DNA damage and of the pathways that lead to it (30), it is quite conceivable to imagine the existence in plants of concerted interactions between different repair enzymes belonging to the same repair machinery or to different repair systems. In keeping with this view, direct interactions between DNA mismatch and nucleotide excision repair enzymes (38), as well as a synergy between base and nucleotide excision repair systems (39, 40), have recently been documented in *S. cerevisiae*. A need for interaction with other protein components can also be anticipated in the case of oxidative DNA damage repair by ZmDP2. In fact, ZmDP2 lacks the kinase activity present in human PNKP that may be required under certain DNA damage conditions to generate ligation-competent 5′-termini at the other end of the break, as well as other activities (*e.g.* DNA polymerase and ligase) that are also required to complete the repair of oxidative DNA damage. In this broader context, the maize 3′-repair phosphoesterase we have identified should be viewed as a functional module of larger, multisubunit repair enzyme complexes rather than as an independent functional unit. Future experiments taking advantage of the molecular reagents reported here will investigate the existence and significance of these interactions in the context of the repair of oxidative damage and other types of DNA damage in plants.

Acknowledgments—We thank Douglas Berg, Yolande Surdin-Kerjan, and Bernard Weiss for the gift of bacterial and yeast strains; Michèle Minet and Dindial Ramotar for plasmids; Stéphane Lobreaux for BMS cells; and Michael Weinfeld for advice on DNA 3′-phosphatase assays. We are grateful to Riccardo Percudani for assistance with sequence analysis and to Alessio Peracchi for helpful discussions on enzyme activity studies. Encouragement and support from Gian Luigi Rossi are also gratefully acknowledged.

REFERENCES

1. Neuwald, A. F., Krishnan, B. R., Brikun, I., Kulakauskas, S., Suziedelis, K., Tomcsanyi, T., Leyh, T. S., and Berg, D. E. (1992) *J. Bacteriol.* **174,** 415–425
2. Gläser, H.-U., Thomas, D., Gaxiola, R., Montrichard, F., Surdin-Kerjan, Y., and Serrano, R. (1993) *EMBO J.* **12,** 3105–3110
3. Murguía, J. R., Bellés, J. M., and Serrano, R. (1995) *Science* **267,** 232–234
4. Murguia, J. R., Belles, J. M., and Serrano, R. (1996) *J. Biol. Chem.* **271,** 29029–29033
5. Peng, Z., and Verma, D. P. (1995) *J. Biol. Chem.* **270,** 29105–29110
6. Gil-Mascarell, R., Lopez-Coronado, J. M., Belles, J. M., Serrano, R., and Rodriguez, P. L. (1999) *Plant J.* **17,** 373–383
7. Quintero, F. J., Garciadeblás, B., and Rodríguez-Navarro, A. (1996) *Plant Cell* **8,** 529–537
8. Spiegelberg, B. D., Xiong, J. P., Smith, J. J., Gu, R. F., and York, J. D. (1999) *J. Biol. Chem.* **274,** 13619–13628
9. López-Coronado, J. M., Bellés, J. M., Lesage, F., Serrano, R., and Rodríguez, P. L. (1999) *J. Biol. Chem.* **274,** 16034–16039
10. Yenush, L., Bellés, J. M., López-Coronado, J. M., Gil-Mascarell, R., Serrano, R., and Rodríguez, P. L. (2000) *FEBS Lett.* **467,** 321–325
11. Miyamoto, R., Sugiura, R., Kamitani, S., Yada, T., Lu, Y., Sio, S. O., Asakura, M., Matsuhisa, A., Shuntoh, H., and Kuno, T. (2000) *J. Bacteriol.* **182,** 3619–3625
12. Bick, J. A., and Leustek, T. (1998) *Curr. Opin. Plant Biol.* **1,** 240–244
13. Varin, L., Marsolais, F., Richard, M., and Rouleau, M. (1997) *FASEB J.* **11,** 517–525
14. Weinshilboum, R. M., Otterness, D. M., Aksoy, I. A., Wood, T. C., Her, C., and Raftogianis, R. B. (1997) *FASEB J.* **11,** 3–14
15. Dichtl, B., Stevens, A., and Tollervey, D. (1997) *EMBO J.* **16,** 7184–7195
16. Cameron, V., and Uhlenbeck, O. C. (1977) *Biochemistry* **16,** 5120–5126
17. Jilani, A., Ramotar, D., Slack, C., Ong, C., Yang, X. M., Scherer, S. W., and Lasko, D. D. (1999) *J. Biol. Chem.* **274,** 24176–24186
18. Karimi-Busheri, F., Daly, G., Robins, P., Canas, B., Pappin, D. J., Sgouros, J., Miller, G. G., Fakhrai, H., Davis, E. M., Le Beau, M. M., and Weinfeld, M. (1999) *J. Biol. Chem.* **274,** 24187–24194
19. Petrucco, S., Bolchi, A., Foroni, C., Percudani, R., Rossi, G. L., and Ottonello, S. (1996) *Plant Cell* **8,** 69–80
20. Wilkinson, J. Q., and Crawford, N. M. (1991) *Plant Cell* **3,** 461–471
21. Sambrook, J., Fritsch, E. F., and Maniatis, T. (1989) *Molecular Cloning: A Laboratory Manual*, Cold Spring Harbor Laboratory, Cold Spring Harbor, NY
22. Laemmli, U. K. (1970) *Nature* **227,** 680–685
23. Ames, B. N. (1966) *Methods Enzymol.* **8,** 115–118
24. Karimi-Busheri, F., Lee, J., Tomkinson, A. E., and Weinfeld, M. (1998) *Nucleic Acids Res.* **26,** 4395–4400
25. Sander, M., and Huang, S. M. (1995) *Biochemistry* **34,** 1267–1274
26. Cunningham, R. P., Saporito, S. M., Spitzer, S. G., and Weiss, B. (1986) *J. Bacteriol.* **168,** 1120–1127
27. Freeling, M., and Walbot, V. (1994) *The Maize Handbook*, Springer-Verlag New York Inc., New York
28. Brocchieri, L., and Karlin, S. (1998) *J. Mol. Biol.* **276,** 249–264
29. Masselot, M., and De Robichon-Szulmajster, H. (1975) *Mol. Gen. Genet.* **139,** 121–132
30. Demple, B., and Harrison, L. (1994) *Annu. Rev. Biochem.* **63,** 915–948
31. Demple, B., Johnson, A., and Fung, D. (1986) *Proc. Natl. Acad. Sci. U. S. A.* **83,** 7731–7735
32. Ramotar, D. (1997) *Biochem. Cell Biol.* **75,** 327–336
33. Gu, L., Huang, S. M., and Sander, M. (1994) *J. Biol. Chem.* **269,** 32685–32692
34. Thaller, M. C., Schippa, S., and Rossolini, G. M. (1998) *Protein Sci.* **7,** 1647–1652
35. Barzilay, G., and Hickson, I. D. (1995) *Bioessays* **17,** 713–719
36. Babiychuk, E., Kushnir, S., Van Montagu, M., and Inze, D. (1994) *Proc. Natl. Acad. Sci. U. S. A.* **91,** 3299–3303
37. Kaneko, T., Katoh, T., Sato, S., Nakamura, A., Asamizu, E., and Tabata, S. (2000) *DNA Res.* **7,** 217–221
38. Bertrand, P., Tishkoff, D. X., Filosi, N., Dasgupta, R., and Kolodner, R. D. (1998) *Proc. Natl. Acad. Sci. U. S. A.* **95,** 14278–14283
39. Xiao, W., and Chow, B. L. (1998) *Curr. Genet.* **33,** 92–99
40. Swanson, R. L., Morey, N. J., Doetsch, P. W., and Jinks-Robertson, S. (1999) *Mol. Cell. Biol.* **19,** 2929–2935

A Plant 3′-Phosphoesterase Involved in the Repair of DNA Strand Breaks Generated by Oxidative Damage

Marco Betti, Stefania Petrucco, Angelo Bolchi, Giorgio Dieci and Simone Ottonello

J. Biol. Chem. 2001, 276:18038-18045.
doi: 10.1074/jbc.M010648200 originally published online February 27, 2001
